

Singular Points and Minutiae Detection in Fingerprint Images Using Principal Gabor Basis Functions

Chih-Jen Lee, Tai-Ning Yang, I-Horng Jeng, Chun-Jung Chen, and Keng-Li Lin

Department of Computer Science
Chinese Culture University
Taipei, Taiwan

Abstract - In the past, most researchers concentrated on the continuity of ridge structures. Because the principal Gabor basis functions (PGBFs) only have large response values with similar orientation and spatial-frequency, a local fingerprint image is represented by a PGBF. We, on the contrast, focus our attention on the discontinuity of ridge structures. This is because the important features (including cores, deltas, and minutiae) are discontinuous to ridge structures. In this paper, we adopt a unified viewpoint to extract cores, deltas, and minutiae by using PGBF-based approach. Fewer steps are applied for important point extraction, and then an efficient approach is implemented. At last, these important points can be classified into cores, deltas, or minutiae by the method of Poincaré index for fingerprint classification or fingerprint matching.

Keywords: Singular points, minutiae detection, principal Gabor basic functions, and fingerprint verification

1 Introduction

Fingerprint patterns are full of ridges and valleys. The information contained in the ridge structures can be treated as three stages. At the coarse stage, the number and the relative positions of the singular points, including cores and deltas, are concerned for classification [1]. At the fine stage, the minutiae, a group of ridge endings and bifurcations, are used as the features for matching [2]. In between the above stages, the middle stage also contains important information, including local ridge orientation (LRO) and local ridge frequency (LRF). Conventionally, only the structures of LROs are used to find the singular points for classification [1] or to enhance ridge structures for minutiae extraction [2].

Gabor filters, simulating visual vertex cells, have the properties of spatial localization, orientation selectivity, and spatial-frequency selectivity [3]. In recent years, therefore, many researchers applied Gabor filters for fingerprint recognition. In [4][5], the Gabor filter-based features were proposed as the fingerprint features to avoid the disadvantages of the minutiae-based approach. This approach used only few steps for fingerprint recognition

and extracted the fingerprint features from raw images directly. In [6][7], Lee et al. used a complete set of Gabor basis functions (GBFs) to demonstrate that the principal GBF (PGBF), which has maximum response over the complete set, can capture the spatial-frequency and orientation of a local fingerprint. In other words, the PGBF and the local fingerprint image have similar spatial-frequency and orientation. Therefore, the input vector of a local fingerprint image is reduced from pixels to an index. After the PGBFs are obtained, the responses of the PGBFs can be used to distinguish fingerprints. This approach not only reduced the features space of fingerprint images, but also increased the accuracy of recognition. Lee et al. also extended this research to fingerprint images enhancement [8], core point detection [9], and minutiae detection [10]. In this paper, we will use a unified viewpoint, based on PGBF, to extract cores, deltas, and minutiae.

2 Local fingerprint images and Gabor basis functions (GBFs)

2.1 Gabor basis functions (GBFs)

The 2-D complete set of GBFs can be expressed as [11]:

$$G_{pqrs}(x, y) = \exp\{-(x-p)^2 + (y-q)^2 / \sigma^2\} \exp[2\pi j(xr + ys) / N_f] \quad (1)$$

where $j = \sqrt{-1}$, $p, q = 0, 1, \dots, N_s - 1$, and

$$r, s = -N_f / 2 + 1, -N_f / 2 + 2, \dots, -1, 0, 1, \dots, N_f / 2 - 1, N_f / 2$$

In the spatial domain, N_s is the number of spatial samples, (p, q) is the spatial window center, and σ decides the extent of spatial windows. In the spatial-frequency domain, N_f is the number of spatial-frequency samples and (r, s) is the location of the frequency center. The angle θ and radial frequency f of GBF are determined by $\tan^{-1}(s/r)$ and $\sqrt{(s/N_f)^2 + (r/N_f)^2}$, respectively. Their relationship on the spatial-frequency plane is demonstrated in Fig. 1. In Eq. 1, we set the number of spatial samples, the number of spatial-frequency samples, and the extents of spatial

windows along x and y axes as the same values for simplification. In the spatial domain, the real components of these basis functions for $N_s = N_f = 16$ are shown in Fig. 2. From Fig. 2, the orientation-selective properties of the GBFs are obvious.

In the spatial-frequency domain, each real GBF (except $r = s = 0$) has twin Gaussian peaks. The envelope of Gaussian function, which is proportional to the reciprocal of σ , determines the channel bandwidths. Various orientations are shown in Fig. 3 (corresponding to 0° , 45° , 90° , and 135°) and the radial frequencies, the distance from the center of the Gaussian function to the origin, are increasing from left to right. Although we only demonstrate some orientations in Fig. 3, in fact, each GBF has twin Gaussian peaks at its frequency center (r, s) . The complete GBFs spread $N_f \times N_f$ Gaussian peaks on the spatial-frequency plane. They only respond to the image with the same orientation and radial frequency as narrowband filters.

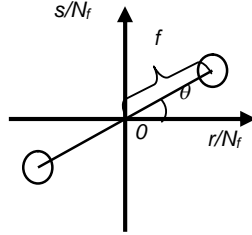


Fig. 1 Parameters of GBF on spatial-frequency plane.

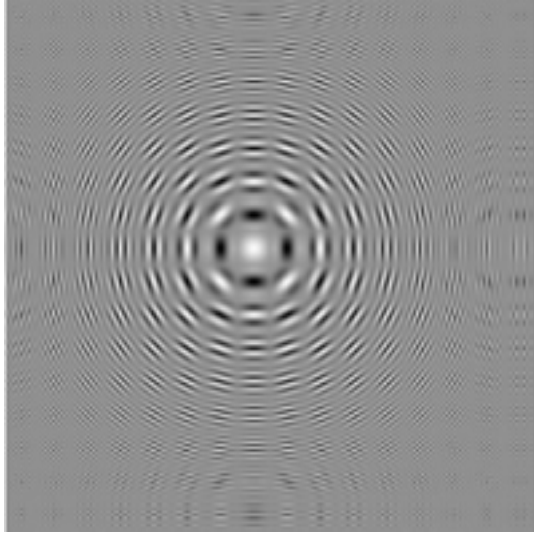


Fig. 2 Real components of complete GBFs.

2.2 Fingerprint images, Gabor responses, and principal GBF (PGBF)

At first, we observe the intrinsic characteristics of fingerprint patterns in the spatial and the spatial-frequency domains. In a local fingerprint image, the LRO and LRF are similar. To analyze the phenomenon of fingerprint

images in the spatial-frequency domain, we transfer these images by Fourier transform and observe their power spectra. Fig. 4(a) shows some local fingerprint images with various LROs. Fig. 5(a) shows some various LRFs with the same orientation.

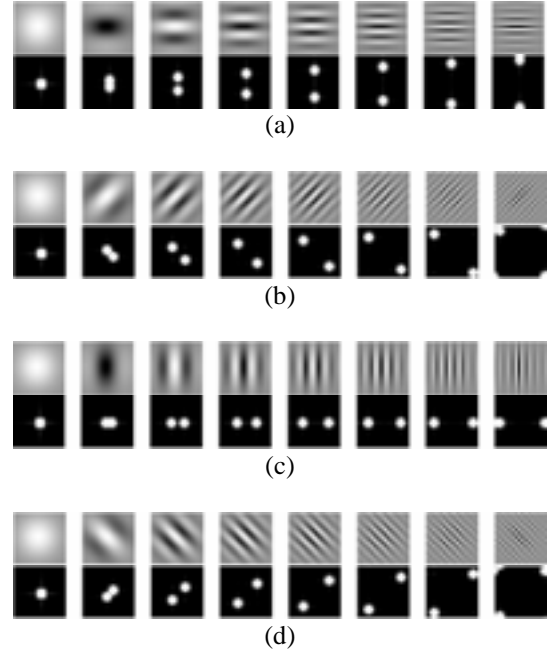


Fig. 3 Power spectra of Gabor filters corresponding to (a) 0° , (b) 45° , (c) 90° , and (d) 135° (the radial frequencies increase from left to right).

The Gabor response R of each GBF corresponding (r, s) is defined as follows:

$$R(r, s) = \left| \sum_p \sum_q I(x, y) G_{pqrs}(x, y) \right| \quad (2)$$

where I is an $N_s \times N_s$ input image. Figs. 4(b) and 5(b) show the corresponding Gabor responses from Figs. 4(a) and 5(a). From Figs. 4(b) and 5(b), the Gabor responses also have twin peaks. This means that the two corresponding GBFs (in fact, they are the same) have the highest responses to the local fingerprint image. Moreover, the orientation and spatial-frequency of the corresponding GBF can represent mainly the local region because the image energy concentrates at its frequency. In other words, a local fingerprint image can be easily captured the main characteristics by using only one GBF. We name it as the principal GBF (PGBF) of the local region. The PGBF is determined by

$$PG = \max_{(r, s)} [R(r, s)]. \quad (3)$$

Because the PGBF can exactly capture the LRO and LRF of a local ridge structures, the dimension of a local fingerprint image is reduced from pixels to only one GBF. A GBF, determined by (r,s) , can also be reduced to an index of the complete GBFs. If a local region has 16×16 pixels, for example, then there are 256 GBFs and the index of the PGBF needs only one byte. That is, the input feature vectors are reduced by a factor of 256.

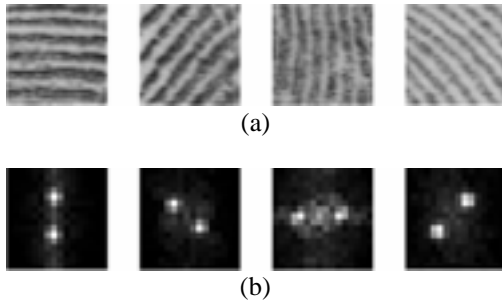


Fig. 4 (a) Original images and (b) responses of GBFs for various LROs.

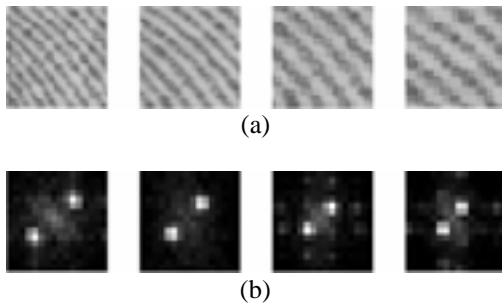


Fig. 5 (a) Original images and (b) responses of GBFs for various LRFs.

3 The discontinuities in fingerprint ridges

In Section 2, we concentrate our attention on the continuities of ridge structures and use PGBF to represent a local fingerprint for the reduction of feature space. This is because, from the view of the middle stage, the ridge structures of fingerprint have similar orientation and frequency in a local region. Therefore, the corresponding PGBF can represent the LRO and LRF of the local region and the response of the PGBF is large. At the fine stage, most ridges are continued, but cores, deltas, and minutiae are discontinued in the ridge structures. So we find that the response of PGBF is large when the ridges are continued; on the contrary, the response is low for minutiae. This is because only one GBF cannot represent the LRO and LRF of the local region with cores, deltas, or minutiae.

Fig. 6 demonstrates the pixel-level responses of PGBFs with core and delta from left to right, and Fig. 7 demonstrates those from various orientations with minutiae.

We can easily find that the positions with the lowest responses from Figs. 6(b) and 7(b) are the positions of core, delta, and minutiae in Figs. 6(a) and 7(a), respectively. So the pixel-level responses of PGBFs can be used to detect the positions of cores, deltas, and minutiae from fingerprint images.

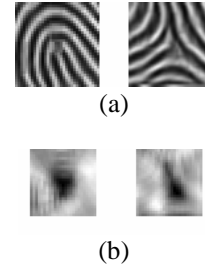


Fig. 6 (a) Original images and (b) pixel-level responses of PGBFs with core and delta from left to right.

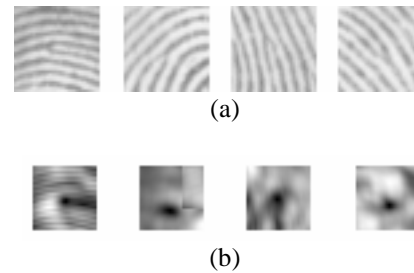


Fig. 7 (a) Original images and (b) pixel-level responses of PGBFs from various orientations with minutiae.

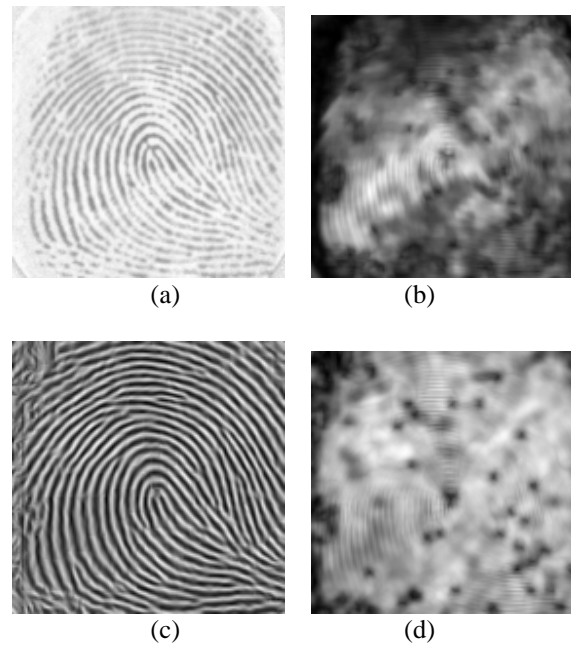


Fig. 8 (a) Original image, (b) the PGBF responses from (a), (c) enhanced image, and (d) the PGBF responses from (c).

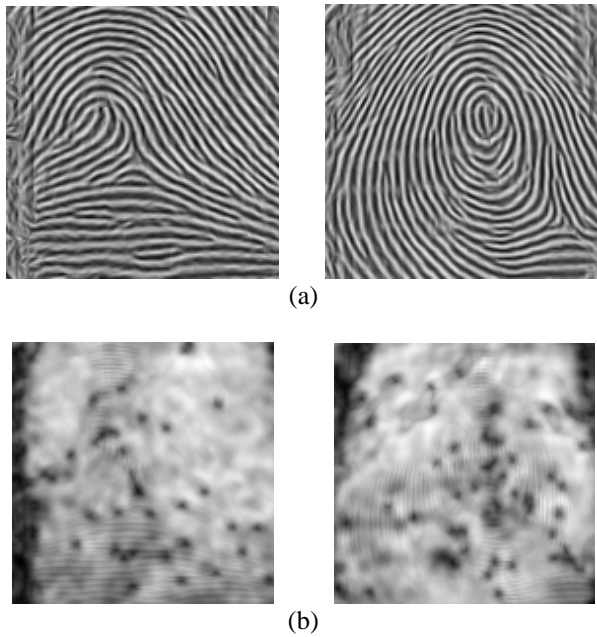


Fig. 9 (a) Enhanced images and (b) the PGBF responses from (a).

Fig. 8(b) shows the responses that we apply the corresponding PGBF of each pixel from Fig. 8(a). The positions of discontinuous ridges, such as core, delta, and minutiae, are darker than their surroundings. But some points are not obvious because their ridge structures are not clear. Therefore we enhance the ridge structure by using the fingerprint enhancement algorithm [8]. Fig. 8(c) shows the enhanced image. We also apply the corresponding PGBF of each pixel on Fig. 8(c), and then Fig. 8(d) is obtained. Comparing Fig. 8(b) and 8(d), we find better result is achieved in the enhanced image. Fig. 9(b) shows other examples from Fig. 9(a). From Figs. 8(d) and 9(b), the darker points might be the important points (such cores, deltas, and minutiae) for fingerprint recognition. But the non-ridge regions are also dark. In the next section, we will discuss how to distinguish these important points from dark regions.

4 Singular points and minutiae extraction

Conventionally, most researchers use Poincaré index [1] to judge whether the singular point exists. To obtain

the structures of LROs, in general, gradient-based method was applied. As for the minutiae detection algorithm, the complex extraction procedure includes image enhancement, orientation estimation, binarization, thinning, and minutiae detection [2]. Based on the same viewpoint, on the contrary, we apply PGBFs on each pixel to check the discontinuity of every ridge structure. The positions of cores, deltas, and minutiae are darker than their surroundings. So these important features are detected by the same method based on the Gabor filter-based approach.

The proposed approach, shown in Fig. 10, includes image enhancement, PGBF detection, binarization, important point detection, and point classification.

Image enhancement and PGBF detection were described in sections 2 and 3. And the corresponding results are shown in Fig. 11(b) and (c), respectively. A global threshold, determined by experiment, is applied to Fig. 11(c), and then the binarized image is obtained, shown in Fig. 11(d). Only the black points will be checked in the following procedure.

Because both the positions of non-ridge regions and discontinuous ridges are dark, it is necessary to check their surrounding's responses. Only the surrounding's responses of discontinuous ridges have high responses; the non-ridge regions do not. This is because the ridge structures of the surrounding of discontinuous ridges are well-defined. Fig. 11(e) shows the important points are detected based on the black points from Fig. 11(d).

After these important points are detected, we will apply the method of Poincaré index [1] to classify their types which are cores, deltas, or minutiae. There are only four values for the following cases:

- 1) 180^0 for core,
- 2) -180^0 for delta,
- 3) 360^0 for whorl, and
- 4) 0^0 for minutia.

Fig. 11(f) shows the detected singular points and minutiae. Fig. 12 also shows some fingerprint images and the corresponding results of detected features.

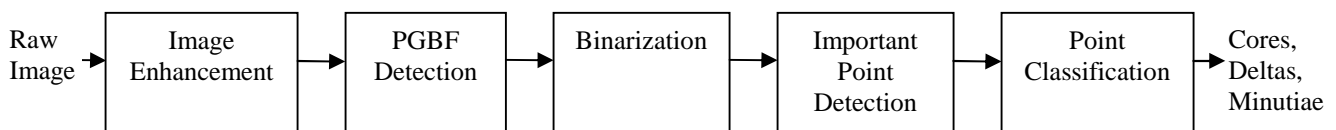


Fig. 10 The proposed approach.

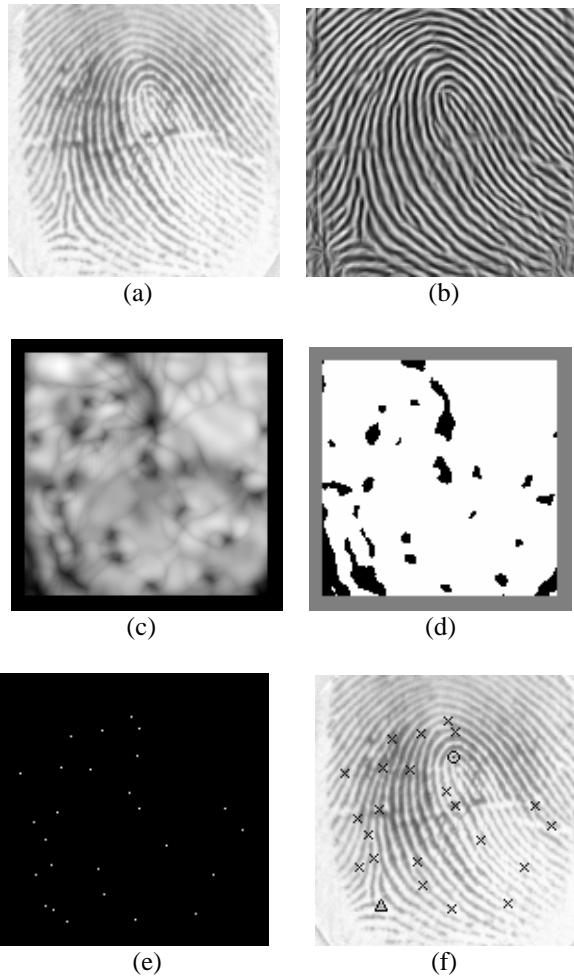


Fig. 11 (a) Original image, (b) enhanced image, (c) PGFBF responses, (d) binarized image, (e) important points, (f) detected singular points and minutiae.

5 Conclusion and further research

Owing to the property that the PGFBFs only have large responses with similar orientation and spatial-frequency, researchers concentrated on the continuity of ridge structures in the past. Now we focus our attention on the discontinuity of ridge structures. That is, important features (including cores, deltas, and minutiae) are discontinuous at the fine stage. Therefore, after the process of PGFBF extraction, the positions of important features would have lower response values than their surroundings.

In this paper, we adopt a unified viewpoint to extract cores, deltas, and minutiae by using PGFBF-based approach. Fewer steps are applied for important point extraction, and then an efficient approach is implemented. At last, these important points are classified into cores, deltas, or minutiae by the method of Poincaré index for fingerprint classification or fingerprint matching.

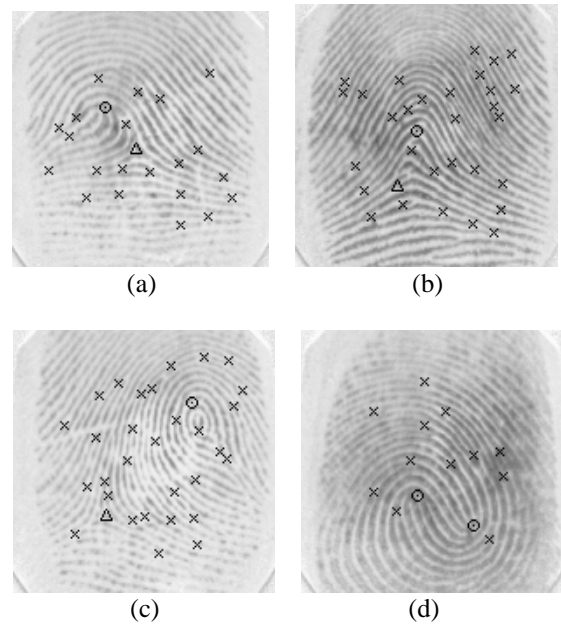


Fig. 12 Some fingerprint images and the results of detected features

Testing with public fingerprint databases, such as the databases from NIST or FVC, is a very important task to show the ability of the proposed approach. We will use the criteria proposed in FVC2002 [12] to evaluate the performance of our approach.

6 Acknowledgements

This work was supported by the National Science Council (NSC), R.O.C. under the project No. 94-2622-E-034-003-CC3.

7 References

- [1] K. Karu and A.K. Jain, "Fingerprint classification," *Pattern Recognition*, Vol. 29, No. 3, pp. 389-404, 1996.
- [2] A.K. Jain, L. Hong, and R. Bolle, "On-line fingerprint verification," *IEEE Trans. Pattern Analysis Machine Intelligent*, Vol. 19, No. 4, pp. 302-314, 1997.
- [3] J.G. Daugman, "Uncertainty relation for resolution in space, spatial frequency, and orientation optimized by two-dimensional visual cortical filters," *J. Opt. Soc. Amer. A*, Vol. 2, No. 7, pp. 1160-1169, 1985.
- [4] C.J. Lee and S.D. Wang, "Fingerprint feature extraction using Gabor filters," *Electronics Letters*, Vol. 35, No. 4, pp. 288-290, 1999.
- [5] A.K. Jain, S. Prabhakar, L. Hong, and S. Pankanti, "Filterbank-based fingerprint matching," *IEEE Trans. Image Processing*, Vol. 9, No. 5, pp. 846-859, 2000.

- [6] C.J. Lee and S.D. Wang, "Fingerprint feature reduction by Gabor basis function," *Pattern Recognition*, Vol. 34, No. 11, pp. 2245-2248, 2001.
- [7] C.J. Lee, S.D. Wang, and Kuo-Ping Wu, "Fingerprint recognition using the responses of principal Gabor basis functions," *Proc. Third International Conference on Information, Communications, and Signal Processing*, Singapore, 2001.
- [8] C.J. Lee and S.D. Wang, "Applying Gabor filters to fingerprint ridge orientation estimation and image enhancement," *Proc. The 2002 International Conference on Imaging Science, Systems, and Technology*, Las Vegas, USA, 2002.
- [9] C.J. Lee and S.D. Wang, "Direct core point detection in raw fingerprint images," *Proc. The 2002 International Conference on Artificial Intelligence*, Las Vegas, USA, 2002.
- [10] C.J. Lee and T.N. Yang, "Direct minutiae detection in raw fingerprint images," *Proc. The 6th IASTED International Conference on Signal and Image Processing*, Hawaii, USA, 2004.
- [11] R.A. Baxter, "SAR image compression with the Gabor transform," *IEEE Trans. Geoscience and Remote Sensing*, Vol. 37, No. 1, pp. 574-588, 1999.
- [12] D. Maltoni, R. Cappelli, J.L. Wayman, and A.K. Jain, "FVC2002: Second Fingerprint Verification Competition," *Proc. 16th International Conference on Pattern Recognition*, Vol. 3, pp. 811-814, 2002.